Chalcogenide Letters Vol. 14, No. 8, August 2017, p. 291 - 295

THE FUNCTION OF BUFFER LAYER IN RESISTIVE SWITCHING DEVICE

B. ZHANG[a], V. PROKOP[a], L. STRIZIK[a], V. ZIMA[b], P. KUTALEK[b], M. VLCEK[b], T. WAGNER[a,c*]
[a]*Department of General and Inorganic Chemistry, Faculty of Chemical Technology, University of Pardubice, Studentska 573, 532 10 Pardubice, Czech Republic*
[b]*Joint Laboratory of Solid State Chemistry of Institute of Macromolecular Chemistry Academy of Sciences of Czech Republic, v.v.i., and University of Pardubice, University of Pardubice, Studentska 573, 532 10 Pardubice, Czech Republic*
[c]*Center of Materials and Nanotechnologies, Faculty of Chemical Technology, University of Pardubice, Nam. Cs. Legii 565, 53002 Pardubice, Czech Republic*

The resistive random access memory is promising to replace the traditional memory technology and the buffer layer plays an important role in chalcogenide based electrolytes. However, there is still lack of convincing experimental result regarding with the mechanism of buffer layer. In this letter, two sets of devices were designed with different position of buffer layer, which proves the buffer layer facilitates the nucleation of Ag filaments.

(Received April 27, 2017; Accepted August 4, 2017)

Keywords: Resistive switching, buffer layer, chalcogenide glass

1. Introduction

The resistive random access memory (RRAM) is promising to replace the traditional memory technology with high scalability and low power consumption [1]. Various geometries of RRAM, such as crossbar, via-hole and atomic switch geometry have been put forward [2]. Among those, crossbar geometry has attracted a lot of attention for its simplicity and ability of integration. Such structure contain inert electrode, counterpart active electrode, buffer layer and cations doped electrolyte, where the conductive filament is formed in electrolyte due to the migration and reduction of cations. The Ag or Cu elements can be used as doping species for oxide layers, such as SiO_2 [3] or chalcogenide layers, such as GeSe [4] or GeS_2 [5]. The buffer layer is often applied in close proximity of chalcogenide electrolyte and its function has been explained by many authors, such as the barrier for the ions migration or the layer for filaments to grow [6-8]. However, there is still lack of convincing experimental result supporting the mechanism.

In this paper, two sets of devices were designed to explore the function of the Al_2O_3 buffer layer; labelled according to the positon of buffer layer: W|Al_2O_3|GeSe:Ag|Ag (INERT BUFFER) and W|GeSe:Ag|Al_2O_3|Ag (ACTIVE BUFFER). And another set of control device was discussed without buffer. The impedance spectrum proves that the buffer layer possesses much smaller electrical resistance compared with chalcogenide electrolyte layer. I-V curves of these two devices show distinct behaviour: diode-like versus resistive switching. We assume that the resistive switching can be related to the incomplete covering of the underlying W layer with Al_2O_3 layer.

*Corresponding author: tomas.wagner@upce.cz

2. Experimental

The INERT BUFFER devices with W|Al_2O_3|GeSe:Ag|Ag stacking was fabricated onto SiO_2 glassy substrate in crossbar geometry (Figure 1(a)). The W electrode was sputtered at initial pressure of $\approx 10^{-4}$ Pa, sputtering power ≈60 W and time 20 minutes through stencil resulting in the thickness of ≈70 nm and line width of ≈100 μm. The Al_2O_3 layer was prepared by pulsed laser deposition (PLD) at initial pressure of $\approx 3.9 \times 10^{-4}$ Pa, pulse energy 215 mJ and deposition time 7 s. The resulting thickness of Al_2O_3 layer was approximately 2 nm on the basis of spectroscopic ellipsometry (Figure 1(b)). The GeSe layer was deposited by thermal evaporation with deposition speed of 1–2 nm s^{-1}; the total thickness was ≈120 nm. Subsequently, a thin layer (≈10 nm) of Ag was deposited by thermal evaporation onto GeSe layer. Afterwards, the device was illuminated by the UV light (peak wave length: λ = 400 nm, intensity: I = 1.25 W cm^{-2}) under an inert N_2 gas environment. The illumination was done with the duration of 1 minute which led to photo-doping of the Ag into GeSe thin layer. The final top Ag electrode was prepared by thermal evaporation (10^{-4} Pa) through stencil to resulting ≈100 nm thickness and ≈100 μm line width; the total cell area is 100 × 100 μm^2 as depicted in Figure 1(c). The ACTIVE BUFFER devices with W|GeSe:Ag|Al_2O_3|Ag stacking was also deposited onto SiO_2 substrate in crossbar geometry (Figure 1(d)). The layer thicknesses and preparation condition were the same as for INERT BUFFER devices. The control device without buffer layer was fabricated without Al_2O_3 buffer layer which the thickness and preparation condition is the same as ACTIVE BUFFER and INERT BUFFER devices (Figure 1(e)).

I-V curve was measured with Keithley 2602, in DC sweep mode. The bias was applied to the top Ag electrode, while the bottom electrode was grounded. The surface topology of W layer and Al_2O_3|W bilayer was measured by the atomic force microscopy (AFM), Solver Pro-M (NT-MDT, Russia) in a semicontact mode. The impedance measurements were carried out on an Auto-lab PGSTAT12 equipped with a FRA2 module, which the W and Ag electrodes of device were replaced with Al as is shown in Figure 1(f). The Al electrodes were deposited by thermal evaporation. And I-t curve of pure Al_2O_3 layer is also measured by the same instrument by applying 0.2 V DC bias.

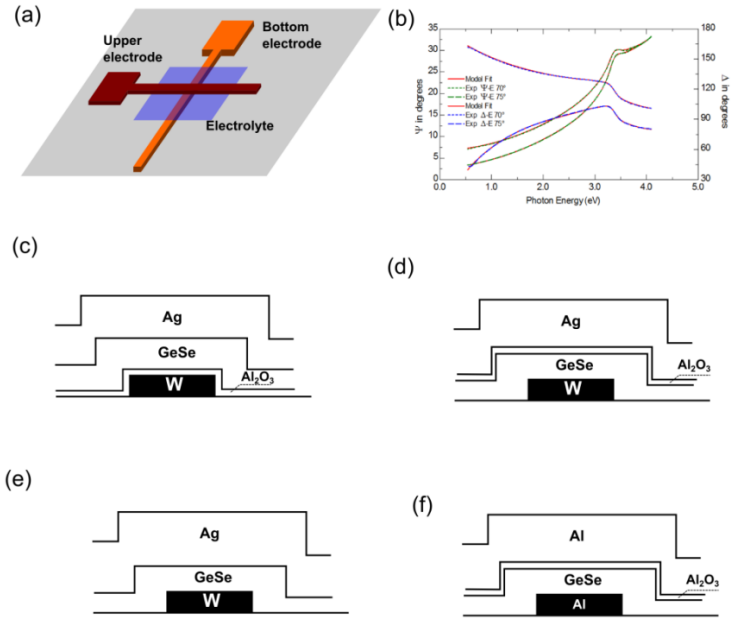

Fig.1 (a) schematic picture of crossbar geometry, (b) ellipsometer result of Al_2O_3 layer for calibration, (c) the cross-section view of INERT BUFFER device, (d) the cross-section view of ACTIVE BUFFER device, (e) the cross-section view of control device without buffer layer,(f) the cross-section view of device for impedance spectroscopy measurement.

3. Results and discussion

Figures 2 (a) and (b) show the AFM surface topography of W layer and Al_2O_3|W bilayer, respectively. One can observe that the particles of Figure 2(b) are wider than those in Figure 2(a) suggesting that the large Al_2O_3 particles do not fully cover the W electrode.

Figure 2(c) describes the impedance data of Al|Al_2O_3|AgGeSe|Al device, the contact resistance Rs is $\approx 10^6\ \Omega$, and the resistance of multilayer is $\approx 10^8\ \Omega$. Figure 2(d) shows the I-t curve ultra thin Al_2O_3 thin layer. Except for the initial two points, the current value is stable, which the stable resistance is approx. $10^3\ \Omega$. Such low resistance can be treated as short circuit through Al_2O_3. In the other words, the Al_2O_3 ultra thin layer does not completely separate the electrodes.

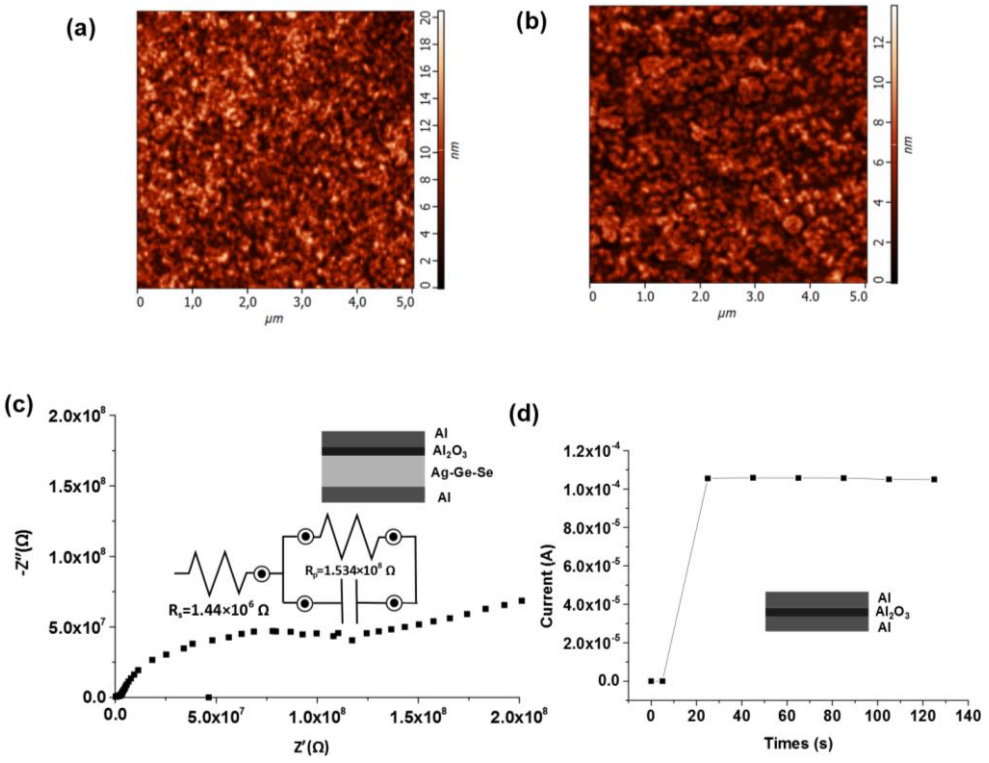

Fig.2 The AFM image of (a) W layer and (b) Al_2O_3|W bilayer, (c) the overall impedance spectrum for Al|Al_2O_3|GeSe:Ag|Al stacked device, and (d) I-V curve of ultra thin Al_2O_3 layer

Figure 3 shows the I-V curve of INERT BUFFER, ACTIVE BUFFER and control device without buffer layer, in which the sweep range and current compliance were set differently. I-V curve of initial two cycles with INERT BUFFER device shows typical resistive switching loop and the SET biases of two cycles are approx. 1.4 V and 1.1 V, respectively (Figure 3(a)). Commonly, the formation of metal or oxygen filament in oxide thin layer needs higher initialization voltage in the first cycle, which is referred as "electroforming" [3]. Nevertheless, the minor difference of SET biases (1.4 V and 1.1 V) in the first two cycles indicates the non-existence of electroforming process in this device, which proves that the metal filament is not formed in Al_2O_3 thin layer. On contrary, the I-V curve in ACTIVE BUFFER device exhibits a diode-like behaviour with current fluctuation and the corresponding threshold bias for current ramping is up to 1.2 V (Figure 3(b)). Moreover, as the compliance of current is not set for ACTIVE BUFFER device, the current shows increasing tendency up to the maximum bias of 3.0 V. Therefore, it can be deduced that no metallic filament is formed in ACTIVE BUFFER device. I-V curve of control device without buffer layer (Figure 3(c)) shows a clear difference, in comparison with the devices with buffer layer (Figure 3 (a), (b)). The 'SET bias' of device without buffer layer is approx. 0.2 V, and the current increases from 10^{-9} to 10^{-6} A. However, it does not exhibit any linear response during

scanning, which can be deduced as no filaments are formed. Therefore, the buffer layer is necessary for resistive switching device.

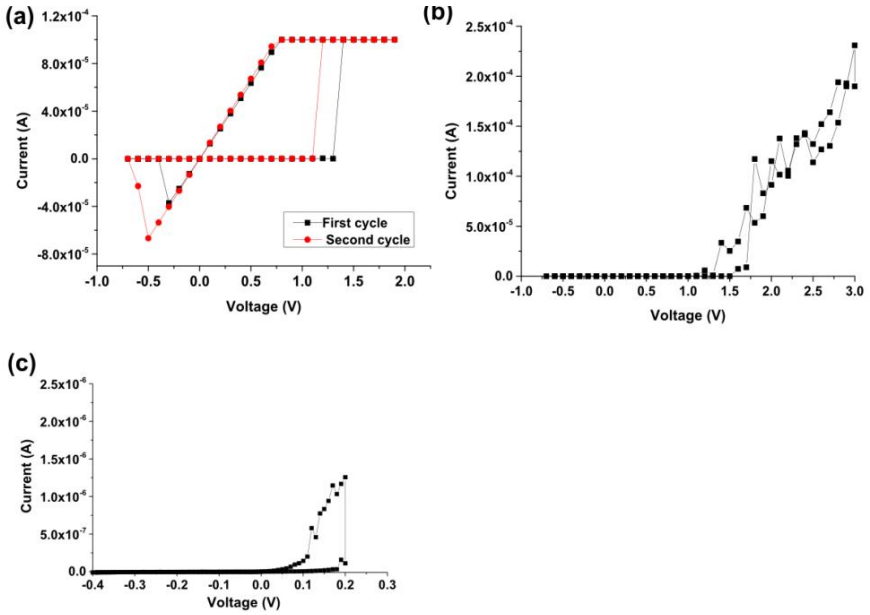

Fig.3 I-V curves: (a) INERT BUFFER, (b) ACTIVE BUFFER, (c) control device without buffer layer.

R. Soni [9] reported buffer layer as an intermedia for filament growth [9] and C. Schindler [6] reported that the buffer layer acts as a diffusion barrier of Ag ions. In our case, we put forward a different explanation. We assume that the function of buffer layer separates the contact electrode area into several small independent regions. Ultrathin Al_2O_3 layer is selected as a buffer material for its less possibility to form the Ag filament [10]. In order to compare the I-V curves, the Ag concentration is kept constant between the INERT BUFFER and ACTIVE BUFFER device using the photo-doping process.

As described above, the positon of buffer layer determines the behaviour of device (resistive switching or diode-like). The proposed mechanism is presented in Figure 4. As the buffer layer in INERT BUFFER device does not completely cover the underlying W thin layer and under reasonable assumption that the filament is not able to be formed within Al_2O_3, one can propose that the Ag^+ ions tend to be nucleated and grew up into Ag filaments at the Al_2O_3 uncovered regions (Figure 4(a)). On the other hand, the buffer layer in ACTIVE BUFFER device lies at the interface of Ag electrode and the GeSe:Ag layer (Figure 4(b)). As the result of that, the Ag ions presented in GeSe layer tend to accumulate near the W electrode causing the polarization. Similar result can be found elsewhere [11]. Therefore, the redox reaction of the required amount of the Ag species is not processed and the cell is turned into a capacitor under bias. The increasing device capacitance leads to larger charging current

.

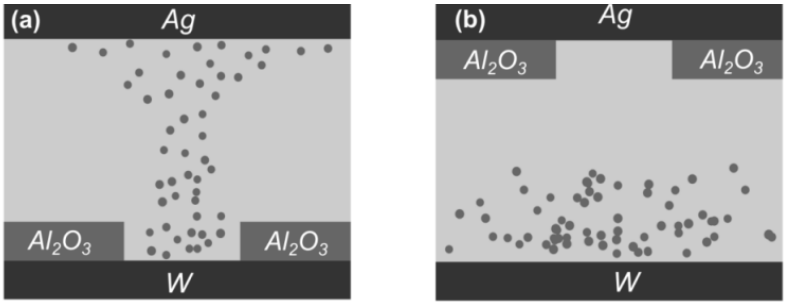

Fig.4 The schematic picture of mechanism in (a) the INERT BUFFER device and (b) ACTIVE BUFFER device, the grey spots represents for Ag ions.

In summary, the creation of filaments with good resistive switching strongly depends on the nucleation. This can be facilitated by introduction of insulating layer at the inert electrode which does not fully cover the electrode. We assume that the creation and growth of separated Ag filaments start from the inert electrode towards the active electrode, which agrees with the TEM observations in Ref. [12].

4. Conclusions

Two devices with different position of buffer Al_2O_3 layer (INERT BUFFER, ACTIVE BUFFER) are designed to study the function of buffer layer. We observed that I-V curves between these two devices are completely different. The increasing current in INERT BUFFER and ACTIVE BUFFER device may be caused by the metal filament formation and capacitance changes, respectively. The buffer layer appreciably facilitates and improves the resistive switching due to controlled nucleation.

References

[1] F. Pan, S. Gao, C. Chen, C. Song, F. Zeng, Mater. Sci. Eng. R Reports **83**, 59 (2014).
[2] R. Waser, R. Dittmann, C. Staikov, K. Szot, Adv. Mater **21** (25), 2632 (2009).
[3] S. Tappertzhofen, I. Valov, T. Tsuruoka, T. Hasegawa, R. Waser, M. Aono, ACS Nano, **7**(7) , 6396 (2013).
[4] M. Kund, G. Beitel, C.-U. Pinnow, T. Rohr, J. Schumann, R. Symanczyk, et al., Proc. IEEE Int. Electron Devices Meet, 754 (2005).
[5] F. Longnos, E. Vianello, C. Carlo, Solid. State. Electron **84**，155 (2013).
[6] C. Schindler, K. Szot, S. Karthäuser, R. Waser, S. Karthauser, R. Waser, Phys. Status Solidi-Rapid Res. Lett. **2** (3)，129 (2008).
[7] B. Zhang, P. Kutalek, P. Knotek, L. Hromadko, J.M. Macak, T. Wagner, Appl. Surf. Sci. 382, 336 (2016).
[8] B. Zhang, M. Fraenkl, J.M. Macak, T. Wagner, Mater. Lett. **163** (15), 4 (2016).
[9] R. Soni, P. Meuffels, A. Petraru, M. Weides, C. Kugeler, R. Waser, et al., J. Appl. Phys. **107** (2), 1 (2010).
[10] D.-T. Wang, Y.-W. Dai, J. Xu, L. Chen, IEEE ELECTRON DEVICE LETT. **37** (7)，878 (2016).
[11] L. Gao, H. Brian, B.S. Dmitri, Phys. Status Solidi - Rapid Res. Lett. **10** (5), 426 (2016).
[12] M.N. Kozicki, A. Tempe, M. Balakrishnan, in: Non-Volatile Mem. Technol. Symp., 7 (2005).